exists for most target nuclei a set of optical-model parameters which describe both the elastic and inelastic scattering of neutrons by nuclei. These parameters vary from nucleus to nucleus, usually by only small amounts. In most cases the effects of additional parameters (if present) and of deformation, etc., are masked by changes in the remaining parameters. These results are purely phenomenological; they are obtained without including several theoretical refinements whose validity we did not attempt to test here.

ACKNOWLEDGMENTS

Computation was done both at the Brookhaven National Laboratory Computation Center and at the Computing Facilities of the Laboratory for Nuclear Science, Massachusetts Institute of Technology. We wish to thank A. Held for checking some calculations. Thanks are due to Mrs. Frances Scheffel, whose assistance in managing the calculations was invaluable.

PHYSICAL REVIEW VOLUME 163, NUMBER 4 20 NOVEMBER 1967

Nuclear-Reaction Studies in the Nickel Isotopes: The $Ni^{61}(p,p')Ni^{61}$, $Ni^{61}(d,d')Ni^{61}$, and $Ni^{60}(d,p)Ni^{61}$ Reactions*

E. R. COSMAN, D. N. SCHRAMM, H. A. ENGE, A. SPERDUTO, AND C. H. PARIS†
Laboratory for Nuclear Science and Department of Physics, Massachusetts Institute of Technology, Cambridge, Massachusetts

(Received 3 March 1967; revised manuscript received 14 June 1967)

The levels of Ni^{61} have been studied with the reactions $Ni^{61}(p,p')Ni^{61}$, $Ni^{61}(d,d')Ni^{61}$, and $Ni^{60}(d,p)Ni^{61}$ at bombarding energies of 7.5 MeV using the MIT-ONR Van de Graaff generator and both the single-gap and multiple-gap spectrographs. The (p,p') reaction seems to be dominated by a compound-nucleus mechanism, and served as a check that we had found all the levels below 4.0 MeV in Ni^{61}. However, the (d,d') transitions to several states below 1.5-MeV excitation were direct and strongly enhanced. In the (d,p) reaction, 197 levels were found below 7.051 MeV in Ni^{61}. The stripping transitions were analyzed with the distorted-wave Born-approximation code JULIE, and resulting neutron single-particle strengths $(2J+1)S_{l_n,j}$, center-of-gravity energies $E_{l_n,j}$, and sum-rule strengths are given. Detailed angular distributions for the nonstripping (d,p) transitions are also given. Most of them have a distinctly oscillatory structure with respect to scattering angle and many are shown to be identical in shape to those found in the $Ni^{58}(d,p)Ni^{59}$ reaction. An averaged strength function is given for these nonstripping states, and it is discussed in terms of intermediate structure. Possible interpretations of the (d,d') and (d,p) results related to the collective and single-particle character of the low-lying states in Ni^{61} are presented.

I. INTRODUCTION

THE present paper is the second in a series concerned with nuclear-reaction studies of the nickel isotopes and describes the excitation of the levels in Ni^{61} by means of the reactions $Ni^{61}(p,p')Ni^{61}$, $Ni^{61}(d,d')Ni^{61}$, and $Ni^{60}(d,p)Ni^{61}$, all at a bombarding energy of 7.5 MeV.

An earlier paper[1] reported the results of the reactions $Ni^{58}(p,p')Ni^{58}$ and $Ni^{58}(d,p)Ni^{59}$. In that study, the use of isotopically pure Ni^{58} targets and high-resolution methods permitted many previously unseen levels to be studied in detail. In the (d,p) case, this revealed the fine structure in the single-particle strength function of the stripping transitions. The sum-rule analysis of these strengths was found to be in fair agreement with shell-model and pairing predictions. In addition, information was obtained on the energies and angular distributions for weaker transitions, henceforth referred to as nonstripping transitions. These nonstripping angular distributions often have well-defined maxima and minima and are not necessarily isotropic or symmetric; however, their over-all patterns are not recognizable as stripping curves for which l values can be assigned. It was speculated that they correspond to levels in Ni^{59} that are populated either by a higher-order (d,p) process, such as core excitation plus stripping, or alternatively by hole-state stripping. To shed more light on this matter, as well as on the validity of a phonon-plus-particle model or other descriptions[2] that have been applied to the odd-A nickel isotopes,[3] it would be desirable to determine the collective character of the nonstripping states, particularly the ones at low excitation energies. This could be done by means of inelastic deuteron scattering; but unfortunately Ni^{59} targets are not available.

* Work supported in part by the U. S. Atomic Energy Commission under Contract No. AT(30-1)-2098.

† Present address: Amersfoort, Holland.

[1] E. R. Cosman, C. H. Paris, A. Sperduto, and H. A. Enge, Phys. Rev. **142**, 673 (1966).

[2] N. Auerbach, Nucl. Phys. **76**, 321 (1966); Phys. Letters **21**, 57 (1966).

[3] L. S. Kisslinger and R. A. Sorensen, Kgl. Danske Videnskab. Selskab, Mat. Fys. Medd. **32**, No. 9 (1960); Rev. Mod. Phys. **35**, 853 (1963); K. Sorensen, Nucl. Phys. **25**, 674 (1961).

Here we have continued this type of investigation by studying the levels in Ni^{61}, which is the only stable odd-mass isotope of nickel. These levels were populated by the three above-mentioned reactions using essentially the same experimental conditions as in Ref. 1. The $Ni^{61}(p,p')Ni^{61}$ reaction was included mainly to identify with some certainty all the levels up to 3.5-MeV extation in Ni^{61}, since it is known that inelastic proton scattering at low energies is relatively insensitive to the nature of the residual nuclear state. The $Ni^{61}(d,d')$-Ni^{61} reaction at these energies, however, enhances states with large collective components and thus provides a tool for identifying collective states in Ni^{61}. This, combined with the results of the $Ni^{60}(d,p)Ni^{61}$ reaction that strongly selects states having large single-particle components, might provide at least a qualitative picture of the structure of the low-lying spectrum. The high resolution, pure targets, and good data statistics made it possible to identify more than twice as many states in Ni^{61} as had been previously reported by other investigators and again allowed the nonstripping angular distributions to be examined in detail.

A distorted-wave Born-approximation (DWBA) analysis of the $Ni^{60}(d,p)Ni^{61}$ reaction (Sec. II C) was carried out utilizing the same optical-model parameters as in Ref. 1. This then resulted in spectroscopic information for Ni^{61} that can be compared with the information for Ni^{59} (Sec. III A). However, shortcomings of this conventional analysis have been accentuated in the present work because the quality of the experimental data is higher. One example of these shortcomings concerns the unclear division between many weak stripping states and what we call the "nonstripping" states. These factors are discussed and their effect on derived sum-rule limits estimated (Sec. III A). Our results are compared to earlier experimental results from (d,p),[4] (p,d),[5] $(n,n'\gamma)$,[6] and other reactions (Sec. III B), and some discussion in terms of nuclear models (Sec. III C) and intermediate structures (Sec. III D) is given.

A DWBA analysis for the (d,d') reaction was not performed here and is deferred to a future paper that will present inelastic-scattering data taken in this laboratory for all stable nickel isotopes.

II. EXPERIMENTAL RESULTS

The 7.5-MeV proton and deuteron beams used in these experiments were provided by the MIT-ONR electrostatic accelerator, and the reaction particles were analyzed in the MIT single-gap and multiple-gap, broad-range magnetic spectrographs.[7,8] The experimental procedure has been described in some detail in Ref. 1.

A. The $Ni^{61}(p,p')Ni^{61}$ Reaction

The target used in this experiment was prepared with enriched Ni^{61} obtained from Oak Ridge National Laboratory, and the isotopic abundances in this material were Ni^{58}, 5.04%; Ni^{60}, 15.56%; Ni^{61}, 74.42%; Ni^{62}, 0.05%; and Ni^{64}, 0.16%. The inelastic protons were recorded in the MIT multiple-gap spectrograph, and a typical spectrum is shown in Fig. 1(a). The yields to the Ni^{61} levels for this 2000 μC of beam exposure are seen to be strong up to 3.6 MeV and fairly nonselective. As mentioned above, this reaction served mainly as a check that all the low-lying states in Ni^{61} had been observed. Indeed, it turned out that all the levels up to 3.5 MeV excited by this mode were also seen in the (d,p) reaction discussed in Sec. II C, and their tabulation is given there.

Figure 2 shows the angular distributions from the (p,p') reaction for the transitions to the lowest ten excited states in Ni^{61}. As expected, they are flat and structureless, supporting the assumption that at this bombarding energy the reaction proceeds mainly by a compound-nucleus mechanism.

B. The $Ni^{61}(d,d')Ni^{61}$ Reaction

The same target was used for this reaction as for the (p,p') case. Figure 1(b) shows the spectrum of deuterons as measured in the multiple-gap spectrograph at $\theta=112.5$ deg. All transitions to levels in Ni^{61} above 2.0 MeV are very weak [Fig. 1(b)], whereas there is a distinct enhancement of a number of groups in the 0.5- to 1.5-MeV range. Also included in the spectrum are the (d,d') transitions to the first 2^+ states in Ni^{58}, Ni^{60}, and Ni^{62}, which were present because of the admixture of these isotopes in the target. Since the percentage composition is known fairly accurately, this information permitted a comparison of the cross sections for these groups relative to those of Ni^{61}.

The angular distributions for the strongest (d,d') transitions below 2.0-MeV excitation in Ni^{61} are shown in Fig. 3. Also, in the lower right-hand corner of the figure is shown the angular distribution from the Ni^{60}-$(d,d')Ni^{60}$ reaction to the first 2^+ state in Ni^{60} at 1.334 MeV. This must be an $l=2$ transfer. In contrast to the (p,p') results, we see in these angular distributions the oscillatory patterns characteristic of a direct-reaction mechanism. Moreover, except for level Nos. 2, 6, 10, and 11, all the Ni^{61} transitions in the figure clearly show patterns very similar to that for the $Ni^{60}(d,d')Ni^{60}$ (2^+). The angular distributions for levels 2 and 6, however, are the same and are characterized by a secondary maximum at 90 deg with marked peaking

[4] R. H. Fulmer, A. L. McCarthy, B. L. Cohen, and R. Middleton, Phys. Rev. 133, 955 (1964).
[5] R. Sherr, B. G. Bayman, E. Rost, M. E. Rickey, and C. C. Hoot, Phys. Rev. 139, B1272 (1965).
[6] R. E. Cote, H. E. Jackson, L. L. Lee, Jr., and J. P. Schiffer, Phys. Rev. 135, B52 (1964).
[7] C. P. Browne and W. W. Buechner, Rev. Sci. Instr. 27, 899 (1956).
[8] H. A. Enge and W. W. Buechner, Rev. Sci. Instr. 34, 155 (1963).

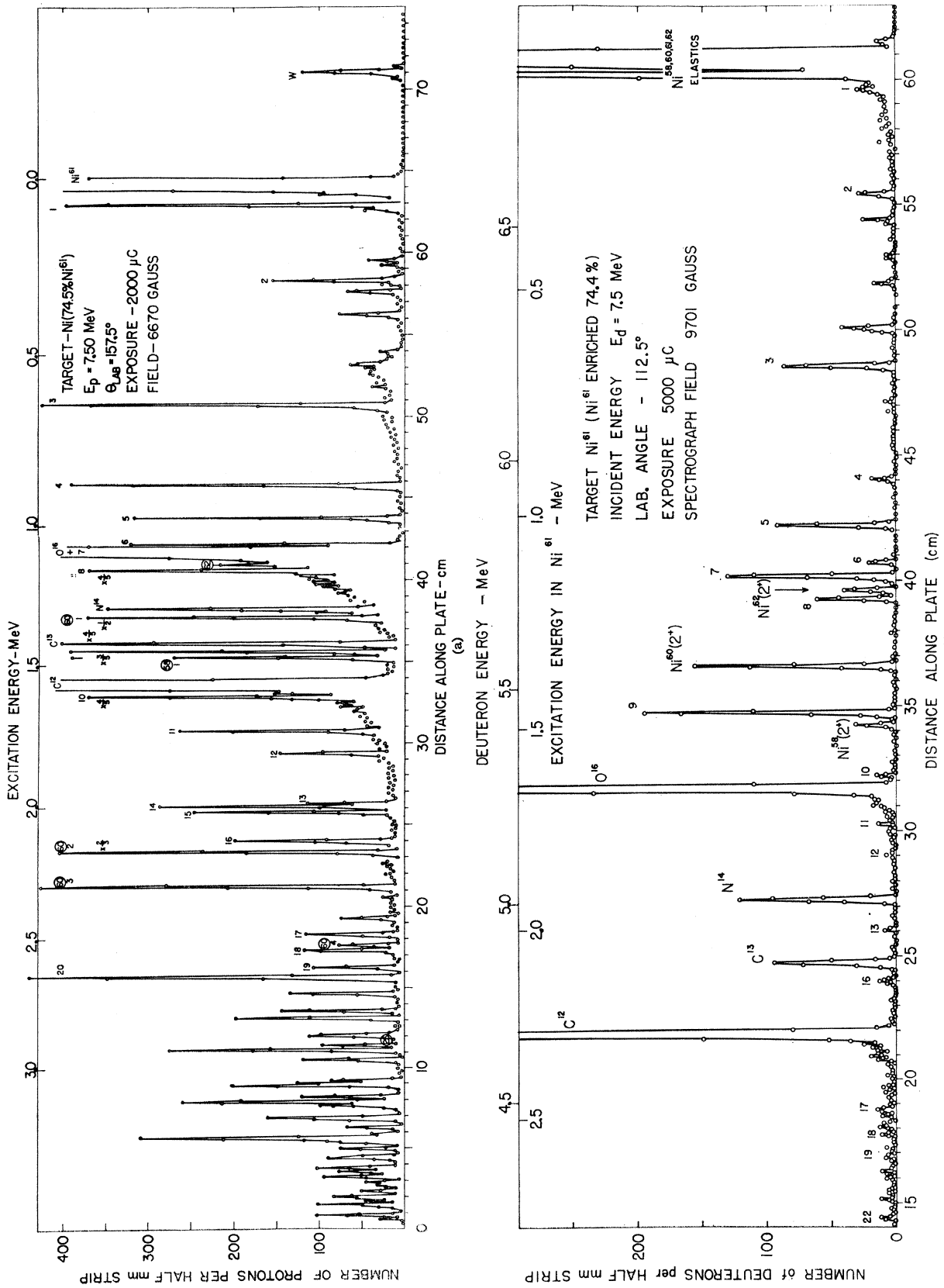

FIG. 1. *(continued)*.

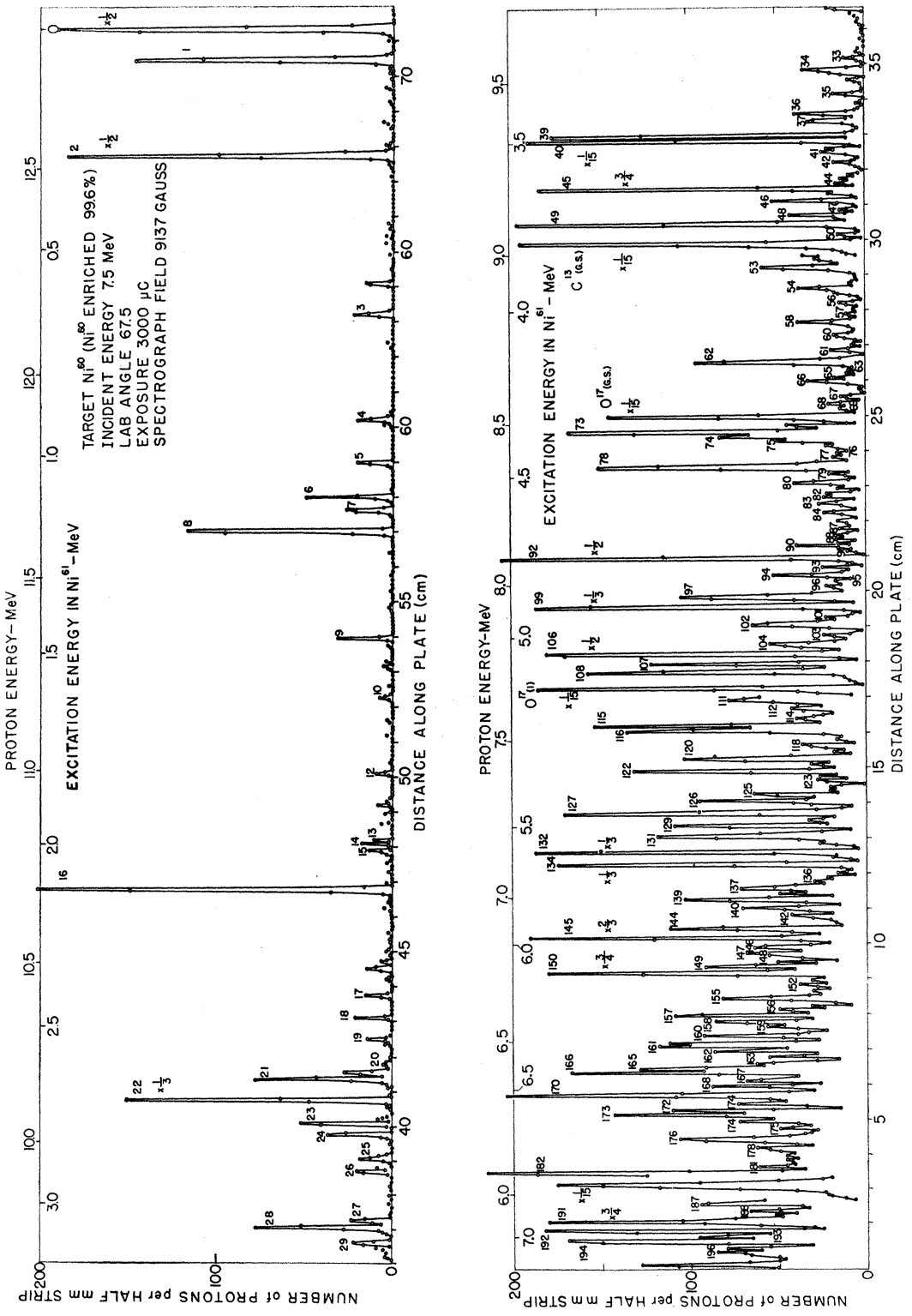

FIG. 1. (a) The proton spectrum from the $Ni^{61}(p,p')Ni^{61}$ reaction at incident proton energy of 7.50 MeV measured at a laboratory angle of $\theta_{lab}=157.5$ deg in the multiple-gap spectrograph. (b) A deuteron spectrum from the $Ni^{61}(d,d')Ni^{61}$ reaction at $\theta_{lab}=112.5$ deg and incident deuteron energy of 7.5 MeV. (c) A typical proton spectrum from the $Ni^{60}(d,p)Ni^{61}$ reaction measured in the multiple-gap spectrograph at $\theta_{lab}=67.5$ deg and incident deuteron energy of 7.5 MeV. As in Figs. 1(a) and 1(b), the peaks are labeled with the numbers used to identify the corresponding states in Ni^{61} listed in Table I.

near 180 deg. The weak group, No. 10, may have an $l=2$ distribution, but the counting statistics are poor and make this assignment inconclusive. Although level No. 11 is also weak, its shape is distinctive and dissimilar to the rest of those shown. Above 1.8 MeV, all the $Ni^{61}(d,d')$ yields were so low that no attempt was made to extract further angular distributions in that region.

C. The $Ni^{60}(d,p)Ni^{61}$ Reaction

Absolute Q values for this reaction were determined from single-gap measurements because of their more accurate energy calibration. The Q value for the ground-state transition in the $Ni^{60}(d,p)Ni^{61}$ reaction was determined to be 5.604 ± 0.008 MeV. The multiple-gap spectrograph was used to obtain angular distributions and establish level identifications with certainty. Figure 1(c) shows a typical proton spectrum measured at 67.5 deg, and Table I summarizes energies and spectroscopic information extracted from the data.

The isotopic analysis of the enriched Ni^{60} target used here was Ni^{58}, 0.8%; Ni^{60}, 99.1%; Ni^{60}, 0.06%; Ni^{62}, 0.02%, and Ni^{64}, 0.006%. The isotopic purity of this target and the long deuteron exposure enabled good counting statistics to be obtained, and thus revealed some of the finer details of the angular distributions, even for the weak and previously poorly studied non-stripping transitions. Figures 4–7 show many of these distributions.

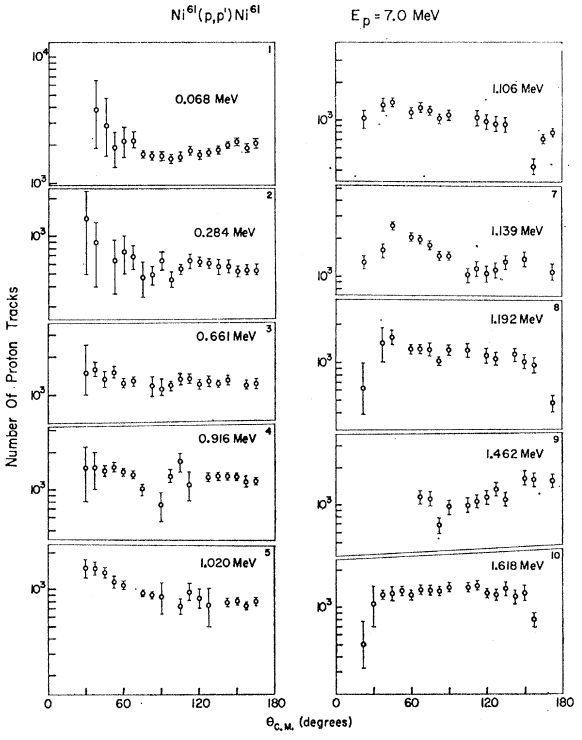

FIG. 2. Angular distributions from the $Ni^{61}(p,p')Ni^{61}$ reaction at 7.50 MeV. The number of the state in Ni^{61} and its excitation energy are indicated in each figure.

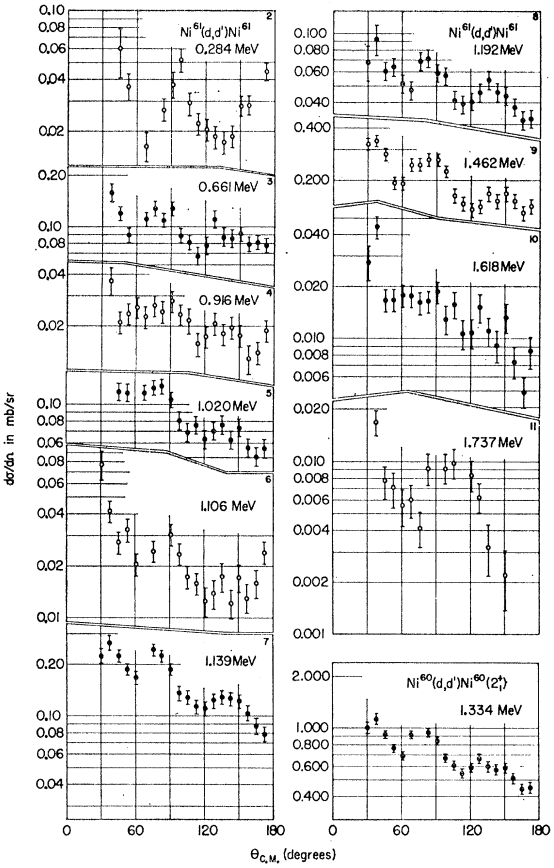

FIG. 3. Angular distributions from the $Ni^{61}(d,d')Ni^{61}$ reaction at 7.50 MeV. Also included in the figure is the angular distribution of the $Ni^{60}(d,d')Ni^{60}$ reaction to the first 2^+ state.

The DWBA analysis of the (d,p) reaction used here proceeds along the same lines as described in Ref. 1. Briefly, the computer code JULIE[9] was used to calculate the reaction function $\sigma(l_n,Q,E_d,\theta)$, where the variables have the usual meaning. The strength $(2J+1)S_{l_n,j}$ was then determined from the experimental cross section $d\sigma/d\Omega$ by use of the relationship

$$d\sigma/d\Omega=1.48(2J+1)S_{l_n,j}\sigma(l_n,Q,E_d,\theta).$$

Here, as usual, $j=l_n\pm\frac{1}{2}$ is the total angular momentum of the captured neutron, and J is the spin of the populated state in Ni^{61}. Since the Ni^{60} target has a 0^+ ground state, we have $J=j$.

[9] R. H. Bassel, R. M. Drisko, and G. R. Satchler, Oak Ridge National Laboratory Report No. ORNL-3240 (unpublished), available from Office of Technical Services, Department of Commerce, Washington 25, D. C. In all the calculations, we neglected finite-range and spin-orbit interactions and placed no lower cutoffs on the radial integrals. The optical-model parameters are the same as those in Ref. 1 and for the deuteron are $V=104$ MeV, $r_0=1.00$ F, $a=0.96$ F, $W=89.8$ MeV, $r_0'=1.41$ F, $a'=0.655$ F, and $r_{0c}=1.3$ F; and for the proton, V=52 MeV, $r_0=1.25$ F, $a=0.65$ F, $W=42$ MeV, $r_0'=1.25$ F, $a'=0.47$ F, and $r_{0c}=1.25$ F. The wave function for the captured neutron was calculated for a Woods-Saxon potential.

TABLE I. Ni^{61} levels up to 7.0 MeV. The first five columns give the results of the present $Ni^{60}(d,p)Ni^{61}$ experiment. The excitation energies in column 2 are arithmetic averages of energies determined at a minimum of three reaction angles. The uncertainties in these values were estimated as ±5-keV standard error for the lowest states and ±10 keV for the highest states. The values of $(d\sigma/d\Omega)_{max}$, l_n, and $(2J+1)S_{l_n,j}$ are given for the levels displaying stripping angular distributions. An "ns" in the column under l_n means that the corresponding angular distribution showed a nonstripping pattern. In many cases there is no clear distinction between a stripping and a nonstripping distribution. In other instances the peaks may have several forward angles obscured by contaminants. When in such a case an l_n value has been assigned, the uncertainty has been indicated by parentheses around the l_n assignment. When two or more levels are so close in energy that the angular distributions could not be extracted separately, they were summed together and bracketed in the table.

Level No.	Present work E_x (MeV)	$(d\sigma/d\Omega)_{max}$ (mb/sr)	l_n	$(2J+1)S$	Fulmer *et al.*[a] E_x (MeV)	l_n	$(2J+1)S$
0	0	3.60	1	1.49	0	1	1.67
1	0.068	0.650	3	3.04	0.069	3	3.37
2	0.284	3.20	1	1.23	0.290	1	1.21
3	0.661	0.151	1	0.053	0.654	1	0.040
4	0.916	0.080	(3)	0.345	0.908	3	0.232
5	1.020	0.029	ns		1.019		
6	1.106	0.345	1	0.108	1.105	1	0.183
7	1.139	0.098	3	0.400	1.139	3	0.271
8	1.192	0.825	1	0.255	1.195	1	0.255
9	1.462	0.105	ns		1.454	3	0.241
10	1.618	0.030	ns		1.622		
11	1.737	0.159	1	0.044	1.750	1	0.027
12	1.814	0.017	ns				
13	1.996	0.021	ns				
14	2.009	0.035	ns				
15	2.025	0.025	ns				
16	2.130	1.480	1	0.392	2.133	1	0.29
		0.965	4	8.450		4	7.1
17	2.417	0.035	ns				
18	2.474	0.058	ns		2.473	(2)	0.006
19	2.536	0.022	ns		2.533		
20	2.602	0.031	ns				
21	2.648	0.369	1	0.087	2.633	1	0.062
22	2.707	1.21	2	0.521	2.694	2	0.53
23	2.773	0.233	1	0.054	2.780	1	0.039
24	2.804	0.090	3	0.291	2.800	3	0.148
25	2.873	0.141	1	0.032	2.876	1	0.018
26	2.910	0.062	(1)	0.014	2.910	2	0.011
27	3.051	0.077	(1)	0.017			
28	3.073	1.80	0	0.067	3.086	0	0.083
29	3.116	0.045	3	0.135	3.127	(2)	0.04
30	3.141	0.021	ns				
31	3.164	0.031	(1)	0.007			
32	3.241	0.052	1	0.011			
33	3.268	0.062	(1)	0.013			
34	3.298	0.211	(1)	0.038	3.305	(3)	0.02
34a	3.308						
35	3.370	0.105	1	0.022			
36	3.427	0.217	1	0.045	3.426	(2)	0.03
37	3.448	0.132	2	0.050	3.448	(2)	0.03
38	3.473	0.031	ns				
39	3.492	0.305	4	2.120			
40	3.507	2.280	2	0.840	3.494	2	1.00
41	3.537	0.045	ns				
42	3.573	0.039	ns		3.567	(2)	0.008
43	3.608	0.049	(ns)				
44	3.628	0.050	ns				
45	3.647	0.53	2	0.196	3.649	2	0.186
46	3.683	0.271	1	0.054	3.679	1	0.045
47	3.708	0.055	ns		3.709		
48	3.725	0.149	1	0.033			
49	3.753	(1.5)	(0)	0.131	3.743	0	0.078
50	3.791	0.096	(1)	0.019			
51	3.819	0.045	(1)	0.009			
52	3.860	0.042	ns				
53	3.879	0.145	(ns)		3.877	2	0.045
54	3.942	0.087	ns		3.923		
55	3.954	0.080	ns				
56	3.984	0.030	ns				
57	4.018	0.034	ns		4.013	2	0.028
58	4.044	0.105	(1)	0.012			
59	4.082	0.036	(ns)		4.088		
60	4.093	0.036	(ns)				
61	4.131	0.076	(0)	0.005			
62	4.163	0.281	2	0.08	4.146	2	0. 070
63	4.189	0.054	2	0.018	4.200		
64	4.200						
65	4.215	0.045	ns				
66	4.226	0.121	(ns)		4.231	1	0.046
67	4.252	0.289	(2)	0.067			
68	4.287	0.095	ns				
69	4.295						
70	4.314	(0.54)	(0)	0.02	4.318		
71	4.336						
72	4.360						
73	4.374	0.76	2	0.284	4.386	2	0.255
74	4.386						
75	4.403						
76	4.425	0.028	ns				
77	4.448						
78	4.476	0.728	2	0.19	4.472	2	0.222
79	4.501						
80	4.522	0.130	(ns)		4.520	1	0.019
81	4.551	0.038	ns				
82	4.569	0.096	(2)	0.030	4.560	0	0.004
83	4.589	0.100	2	0.032	4.582	0	0.004
84	4.605	0.039	ns				
85	4.623	0.065	ns				
86	4.635		ns				
87	4.650	0.035	ns				
88	4.665	0.043	ns				
89	4.694		ns				
90	4.716	0.099					
91	4.736				4.727	1	0.008
92	4.762	2.69	2	0.958	4.760	2	0.55
93	4.795	0.042	ns				
94	4.818	0.130	(ns)		4.82	0	0.012
95	4.837	0.045	ns				
96	4.857	0.080	(1)	0.015			
97	4.872	0.50	(0)	0.052	4.877	2	0.072
98	4.883						
99	4.916	(10.0)	0	0.40	4.907	0	0.25
100	4.954						
101	4.968	0.385	2	0.098	4.970	2	0.071
102	4.980						
103	5.005	0.080	(ns)				
104	5.020	0.034	ns				
105	5.034	0.115	(1)	0.021			
106	5.064	(4.51)	0	0.163	5.070	0	0.160
107	5.097	0.280	1	0.054	5.100	2	0.062
108	5.121	0.590	1	0.108	5.134	1	0.059
109	5.168	0.086	ns				
110	5.187	2.98	0	0.102	5.200	0	0.115
111	5.216	0.170	2	0.053	5.23	2	0.057
112	5.241	0.100	ns				
113	5.263						
114	5.280	0.157	ns				
115	5.295	0.190	(1)	0.033			
116	5.309	1.192	0	0.053			
117	5.336	0.025	ns		5.318	2	0.155
118	5.356	0.140	(1)	0.024	5.378	(1)	0.007
119	5.366	2.40	(0)	0.071	5.413	2	0.081
120	5.395						
121	5.405						
122	5.440	0.390	1	0.070	5.453	2	0.092
123	5.466	0.067	ns				
124	5.487	0.047	ns				
125	5.512	0.160	(ns)				

TABLE I. (*continued*).

Level No.	E_x (MeV)	Present work $(d\sigma/d\Omega)_{max}$ (mb/sr)	l_n	$(2J+1)S$	Fulmer *et al.*[a] E_x (MeV)	l_n	$(2J+1)S$
126	5.534	0.278	2	0.071	5.537	2	0.076
127	5.574	0.510	1	0.090	5.566	2	0.102
128	5.601	0.574	ns		5.608	2	0.064
129	5.620	0.276	2	0.072			
130	5.645	0.284	(1)	0.052	5.647	2	0.098
131	5.659	0.30	1	0.049			
132	5.703	2.14	2	0.521	5.703	2	0.375
133	5.723						
134	5.742	1.318	2	0.325	5.742	2	0.265
135	5.796	0.225	(ns)				
136	5.804						
137	5.821	0.179	(ns)				
138	5.842	0.099	ns				
139	5.859	0.280	(0)	0.034	5.860	2	0.052
140	5.883	0.162	(ns)				
141	4.894	0.103	(2)	0.028	5.89	2	0.036
142	5.914						
143	5.934	0.382	2	0.098	5.95	2	0.017
144	5.957						
145	5.987	1.09	0	0.071	5.98	2	0.060
146	6.016	0.130	(2)	0.037	6.00	0	0.101
147	6.041	0.192	(ns)		6.035	(2)	0.013
148	6.072	$\leqslant$0.035	ns				
149	6.085	0.150	(2)	0.038	6.073	2	0.035
150	6.102	0.781	2	0.192	6.099	2	0.205
151	6.135						
152	6.148	0.040	ns				
153	6.166	0.030	ns		6.168		
154	6.176	0.179	ns				
155	6.184						
156	6.227	0.090	(ns)				
157	6.249	0.275	(2)	0.071	6.263	2	0.077
158	6.269	0.144	ns				
159	6.289	(0.138)	(0)	0.015			
160	6.314	0.185	ns				
161	6.346	0.492	2	0.115	6.320	2	0.056
162	6.371	0.231	2	0.053	6.363		
163	6.391	0.060	ns		6.389	(2)	0.085
164	6.413	(0.120)					
165	6.427	0.916	2	0.213	6.40	2	0.189
166	6.444						
167	6.471	0.173	(ns)		6.448	2	0.312
168	6.492	0.165	ns				
169	6.515	0.296	(1)	0.045	6.531		
170	6.538						
171	6.556	0.115	ns		6.543		
172	6.571	0.403	(2)	0.094			
173	6.589						
174	6.609	0.140	2	0.029	6.609		
175	6.630						
176	6.661	0.400	2	0.091	6.700	2	0.072
177	6.676						
178	6.706						
179	6.732						
180	6.748				6.727		
181	6.767						
182	6.776				6.800	2	0.102
183	6.803						
184	6.818						
185	6.838						
186	6.849						
187	6.878						
188	6.908				6.892	(2)	0.076
189	6.923						
190	6.928				6.924		
191	6.939						
192	6.971				6.97		
193	6.993						
194	7.008				7.019		
195	7.036						
196	7.051						

[a] Reference 4.

III. DISCUSSION

A. Level Schemes, Spectroscopic Factors, and Sum Rules

Below 7.0 MeV we observed 193 levels in Ni^{61} with the (d,p) reaction, compared with 148 levels in Ni^{59} (Ref. 1). This increase was expected because the number of valence neutrons outside the $N=28$ shell is increased. Figure 8 shows a comparison of the level schemes of Ni^{58}, Ni^{59}, Ni^{60}, and Ni^{61} below 4.0 MeV derived from our data. Columns 2 and 5 show only the states for which the transitions have nonstripping (ns) patterns; thus, they are transitions that have small single-particle components. Although the total level density is increased from Ni^{59} to Ni^{61}, the number of nonstripping states in the low-lying spectrum is decreased by 15%. This suggests that the lowest single-particle states in Ni^{61} are being mixed more strongly among the more complicated configurations than in Ni^{59}. Figure 9 also illustrates this trend. The figure gives the strength functions $(2J+1)S_{l_n,j}$ for transitions with $l=0$, 1, 2, 3, and 4 plotted against excitation energy. In going from Ni^{59} to Ni^{61} there is an increase in the number of $l=3$ and $l=4$ fragments, as well as an increase in the density of states with $l=0$ and $l=2$ transitions. Although the number of $l=1$ states has remained constant at 33, the lowest four large $l=1$ fragments have a larger energy spread in Ni^{61} than in Ni^{59}, and the numerous weak higher $l=1$ states are at lower energies in Ni^{61} than in Ni^{59}.

In the sum-rule analysis that is carried out below there are two sources of ambiguities in addition to the uncertainties inherent in the DWBA analysis which this study has emphasized. First, as mentioned earlier, there is no clear dividing line between stripping and nonstripping patterns. In Figs. 4, 5, and 6, there are numerous examples of transitions where the data fit the DWBA curve reasonably well for the first forward-angle maximum but deviate strongly from it otherwise. In these cases, tentative l_n values are given in parentheses in Table I. For those transitions where there is no resemblance to any DWBA stripping curve even in the forward angles, a designation of nonstripping has been given in Table I. Level Nos. 96, 105, 107, 108, and 115 in Fig. 5 illustrate this type of ambiguity with what appears to be a trend from a weak state showing similarity to the $l_n=1$ pattern in the forward angles but departing radically in the back angles through a strong

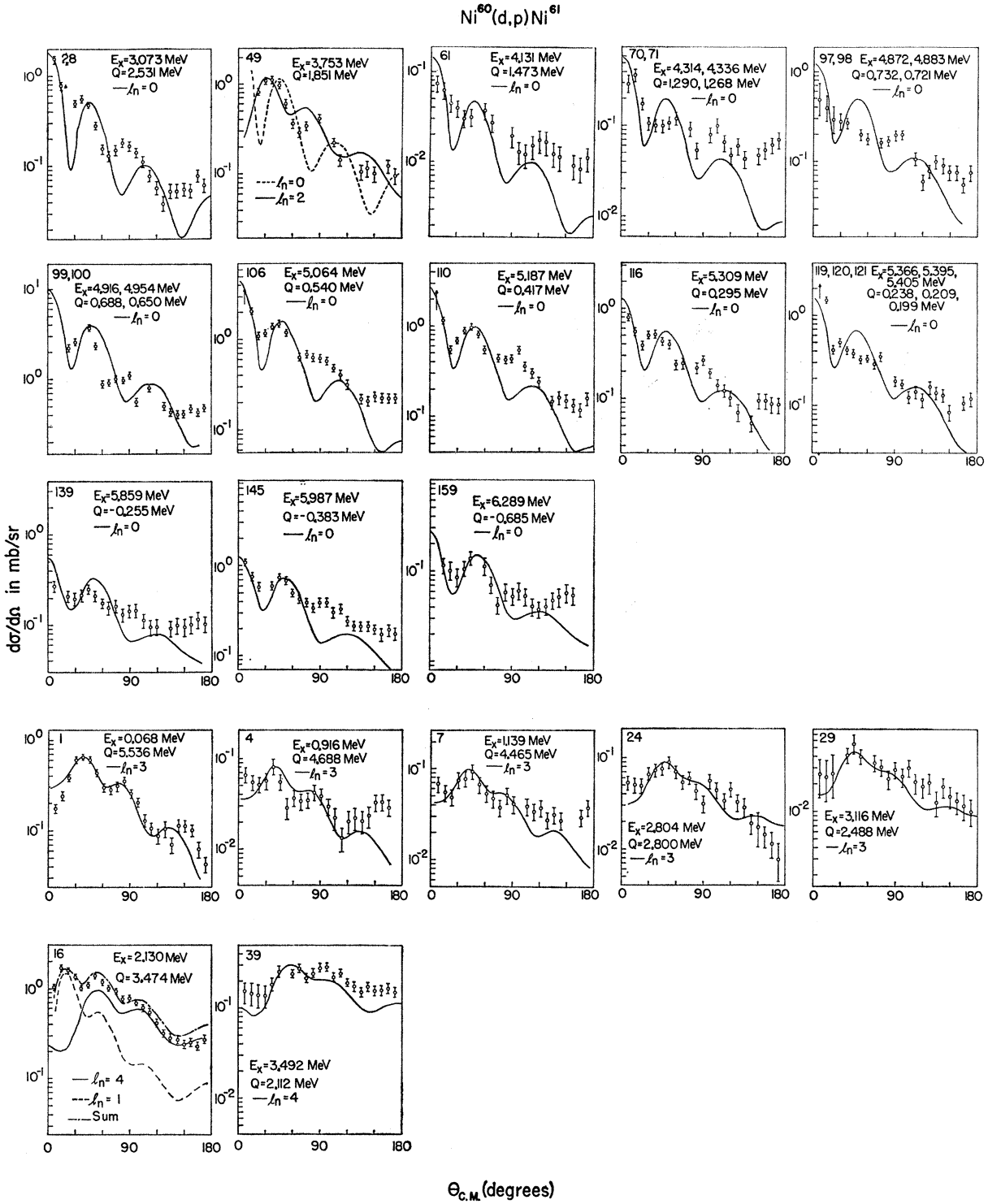

FIG. 4. Angular distributions of $Ni^{60}(d,p)Ni^{61}$ transitions are shown here which appear to have either $l_n=0$, 3, or 4 patterns. At the top left of each drawing is the number used to identify the corresponding state in Table I. Also, the excitation energy E_x and Q value for each transition are indicated. The circles represent the experimental data, the vertical bars give the statistical errors, and the solid curves are derived from DWBA calculations assuming they indicate l_n and Q values.

and characteristic $l_n=1$ shape (No. 108), and back to the weaker-type state again. In this case, it seems unclear whether to assign $l_n=1$ to state Nos. 96, 105, and 115, and, if so, how to extract a spectroscopic factor.

The second source of ambiguity in the sum-rule

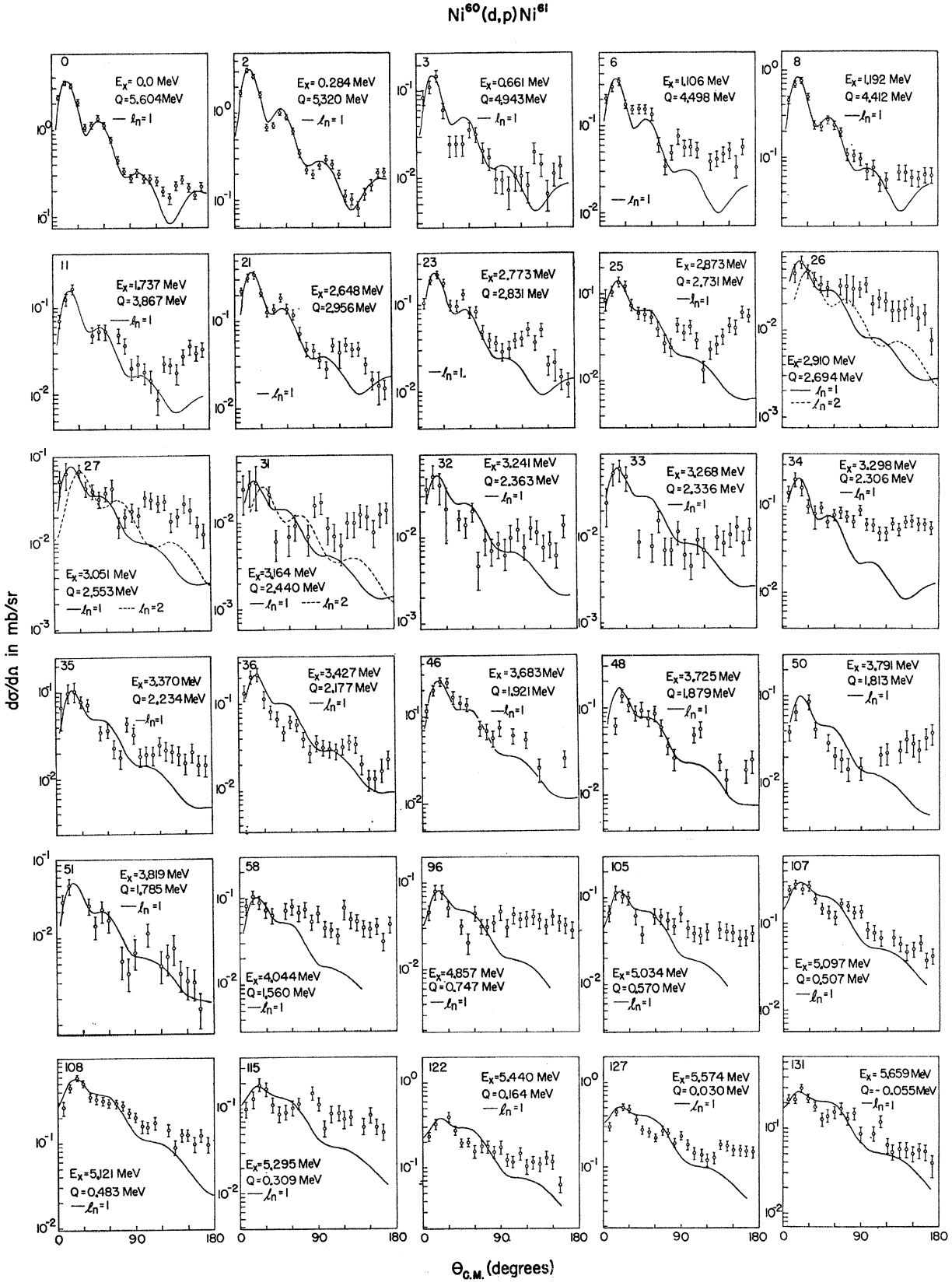

FIG. 5. $Ni^{60}(d,p)Ni^{61}$ angular distributions that suggest an $l_n = 1$ neutron capture.

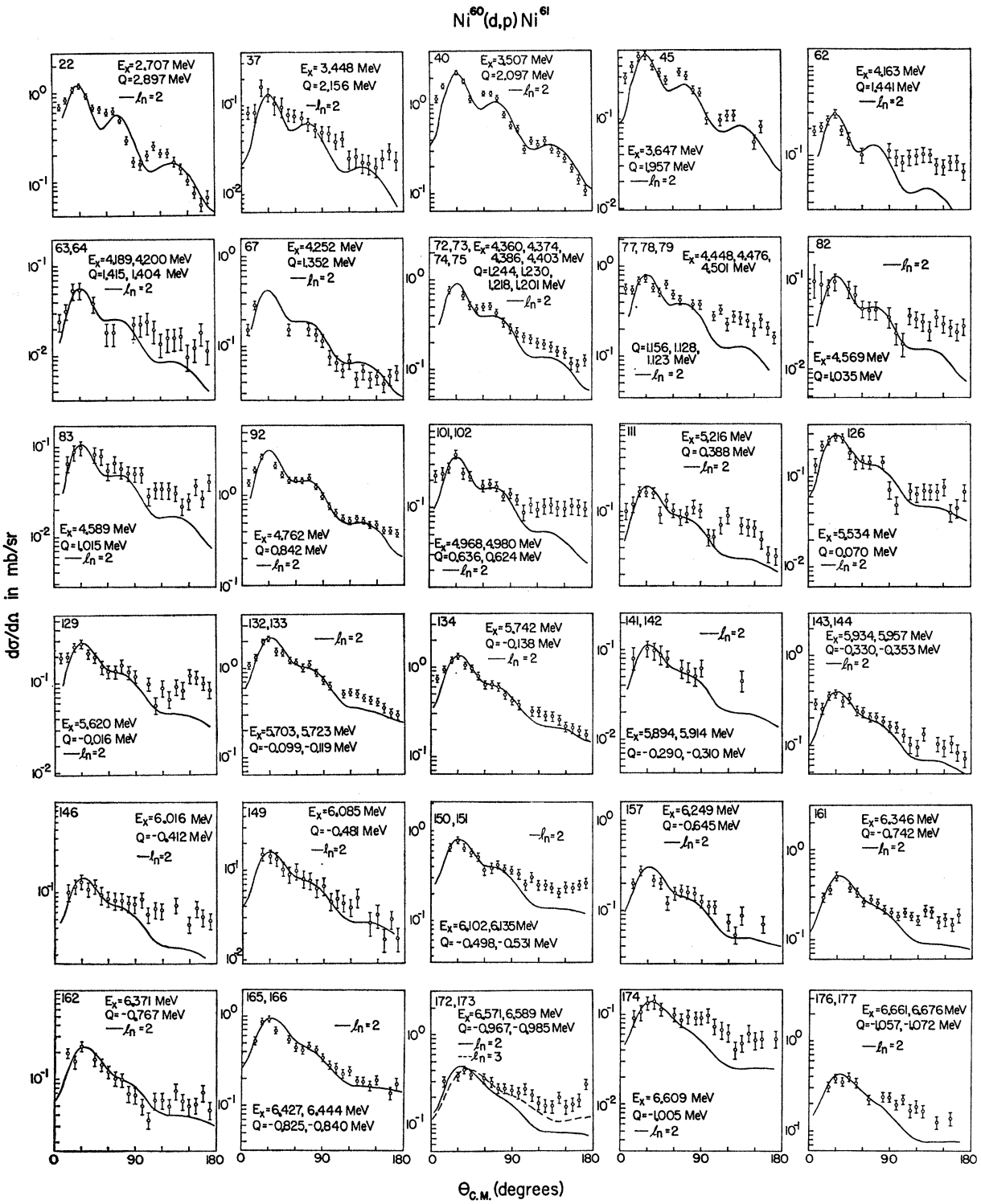

FIG. 6. $Ni^{60}(d,p)Ni^{61}$ angular distributions that suggest an $l_n=2$ neutron capture.

analysis is that some of the weak transitions assigned $l_n=(1)$ in this work and also in the $Ni^{58}(d,p)Ni^{59}$ case[1] may be due to configurations other than $2p$; for instance, stripping to holes in the $f_{7/2}$ orbit (see the discussion in Sec. II B and also in Ref. 1, Sec. V B). If such an anomalous behavior existed at this bombarding energy, it would be an error to include such states in calculating the $2p$ strength. We believed that it was justifiable,

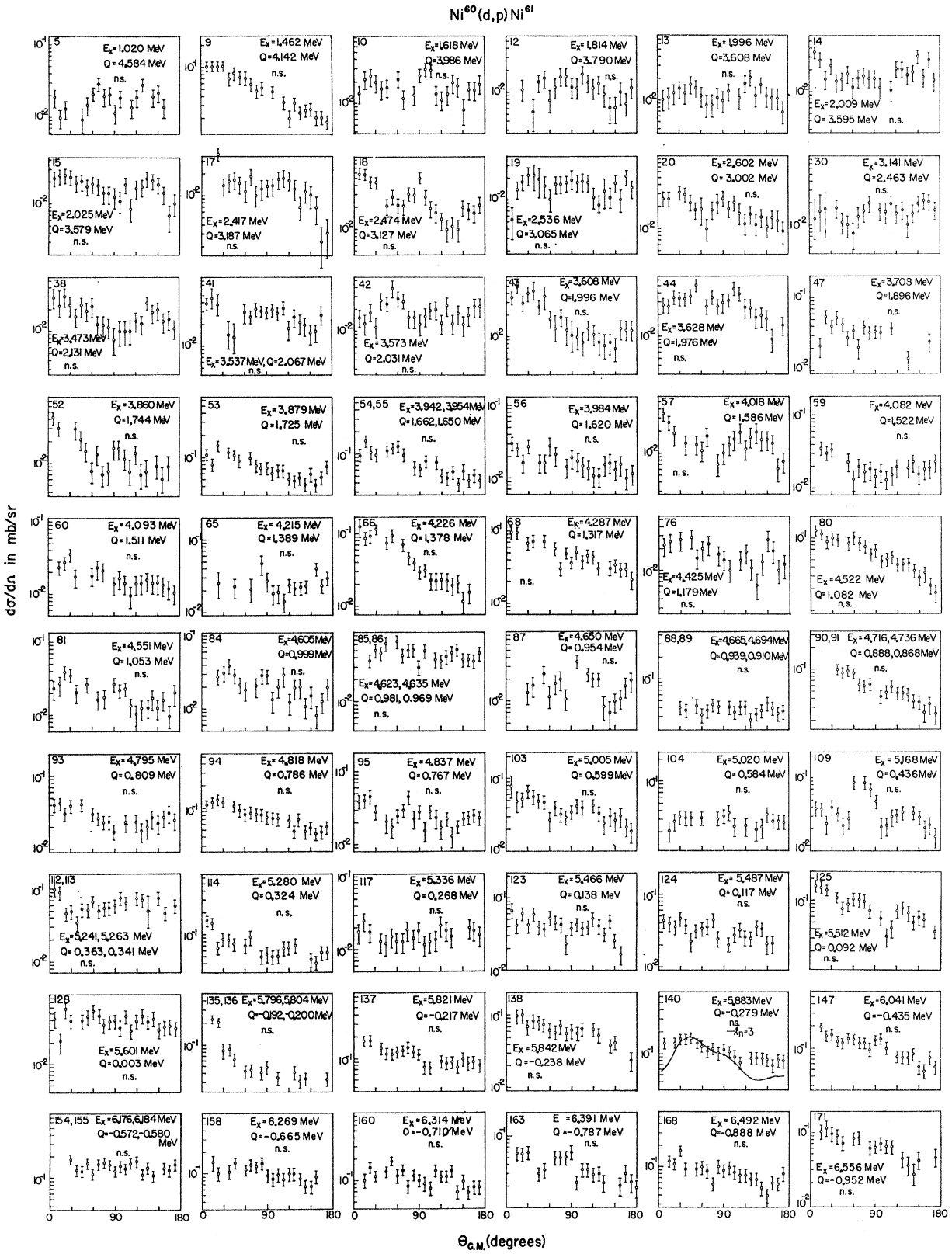

FIG. 7. $Ni^{60}(d,p)Ni^{61}$ angular distributions whose patterns deviate markedly from usual stripping patterns and which have been classified as nonstripping (ns) transitions.

therefore, to show most of the angular distributions here in order that the reader might evaluate for himself the assignments we have made in Table I.

Table II shows the sum strengths calculated for $Ni^{58}(d,p)Ni^{59}$ (Ref. 1) and the present results for $Ni^{60}(d,p)Ni^{61}$. Since J^π of $Ni^{60}(0)$ is 0^+, the interpretation of these values is given by[10]

$$\Sigma(2J_f+1)S_{l_n,j} = \text{number of } (l_n,j) \text{ neutron holes in the target.}$$

In order to estimate the size of the error possible from the above uncertainties, as well as from uncertainties caused by insufficient data, we have calculated two sums for each orbit. The first, case (a) in Table II, includes all levels for that orbit whether or not the l_n assignment is tentative, and the second, case (b) in Table II, includes all except the tentative assignments (in parentheses in Table II of Ref. 1 and Table I of this paper).

In Ni^{61}, as in Ni^{59}, the $2p$ strength observed appears to be too large for both methods of taking the sum strength, (a) and (b). However, the discrepancies are not outside the uncertainties in the DWBA analysis. We find closest agreement to theory by assuming all $l_n=3$ transitions, certain or not, as being $f_{5/2}$ stripping [case (a)]; whereas, by neglecting the distribution No. 3 showing some departure from DWBA-predicted shapes, we obtain a lower limit to the $f_{5/2}$ strength present [case (b)]. The discussion of possible nonclosure of the $f_{7/2}$ shell is deferred to Sec. III B. Our data revealed only one $g_{9/2}$ level in Ni^{59} and two in Ni^{61} with the $(2J+1)S_{l,j}$ strengths remaining constant at 10.6, corresponding to completely vacant orbits in the target nuclei. It is also evident from the table that some of the $s_{1/2}$ and $2d$ strengths lie outside the energy range of the experiment.

TABLE II. Sum of spectroscopic strengths $\Sigma(2J+1)S_{l_n,j}$. It is assumed here that the $l_n=0$, 1, 2, 3, and 4 transitions correspond to the orbits $3s$, $2p$, $2d$, $1f_{5/2}$, and $1g_{9/2}$, respectively. The sum has been calculated from the data in two ways, described in the text. Pairing-model predictions are taken from Ref. 3. The $(\nu=1)$ calculation refers to results from Ref. 2. Simple shell-model values correspond to the oversimplified limit of exactly two extra core neutrons in the $2p_{3/2}$ orbit for Ni^{58} and four neutrons in the $2p_{3/2}$ orbit for Ni^{60}.

$Ni^{58}(d,p)Ni^{59}$		$2p$	$1f_{5/2}$	$1g_{9/2}$	$3s_{1/2}$	$2d$
Experiment	Case (a)	6.6	5.2	10.6	0.96	4.5
	Case (b)	6.2	4.8	10.6	0.94	4.1
Pairing theory		4.6	5.4	9.9	2.0	10.0
$(\nu=1)_{\text{calc}}$		4.6	5.4	...	...	...
Shell model		4.0	6.0	10.0	2.0	10.0
$Ni^{60}(d,p)Ni^{61}$						
Experiment	Case (a)	4.6	4.2	10.6	1.18	5.5
	Case (b)	4.3	3.9	10.6	0.86	5.1
Pairing theory		3.5	4.5	9.9	2.2	10.0
$(\nu=1)_{\text{calc}}$		3.5	4.5	...	...	...
Shell model		2.0	6.0	10.0	2.0	10.0

[10] M. H. Macfarlane and J. B. French, Rev. Mod. Phys. 32, 567 (1960); S. Yoshida, Nucl. Phys. 38, 380 (1962).

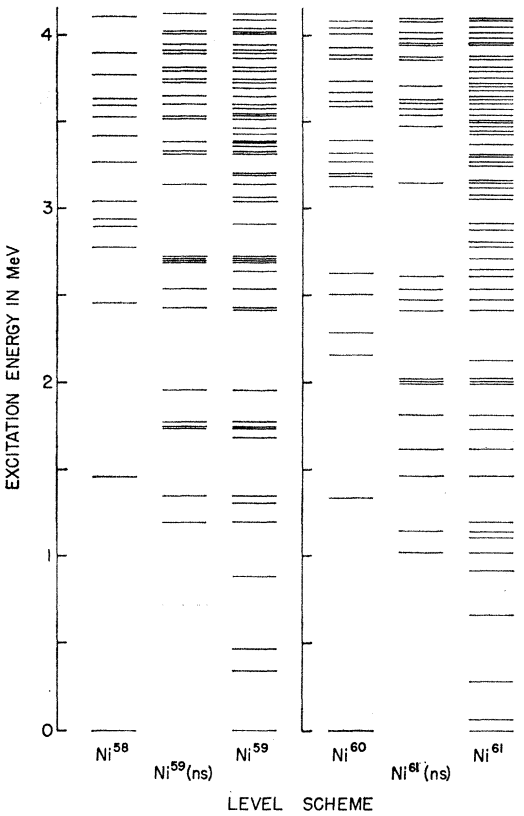

FIG. 8. The energy spectra of Ni^{58}, Ni^{59}, Ni^{60}, and Ni^{61} below 4.1 MeV. The Ni^{58} and Ni^{60} levels shown were determined by (p,p') reactions done in this laboratory, and the Ni^{59} and Ni^{61} levels are all those found from the (d,p) reactions reported in Ref. 1 and the present work, respectively. The center columns show the positions of nonstripping (ns) levels, also from the (d,p) reactions.

As another variation on the usual DWBA analysis, we have applied the fixed Q value "effective-binding" prescription to the present data. This is described in Refs. 1 and 5. Briefly, in the DWBA calculation, a constant separation energy is fixed equal to the single-particle energies for each of the classes of states $j=l_n+\frac{1}{2}$ and $j=l_n-\frac{1}{2}$ instead of varying the neutron well depth to achieve the correct separation energy for each state in the residual nucleus. Since the spins of most of the $l_n=1$ levels have not been measured, we have had to make somewhat arbitrary divisions into $j^\pi=\frac{3}{2}^-$ and $\frac{1}{2}^-$ levels. The results of this analysis are shown in Table III, and their sensitivity to these divisions is estimated by considering three widely differing distributions of spins, cases (1), (2), and (3), specified in the caption of Table III. Once again the effect on the sum strengths of including and excluding the uncertain $l_n=1$ and $l_n=3$, assignments is indicated by the values shown under (a) and (b) of Table III, respectively.

For the cases presented, the results of Table III show that the ambiguities of unknown spins and tentative $l_n=1$ assignments affect most strongly the $p_{1/2}$ sum strength and the relative positions of the $p_{3/2}$, $p_{1/2}$, and $f_{5/2}$ single-particle energies. For both reactions, the

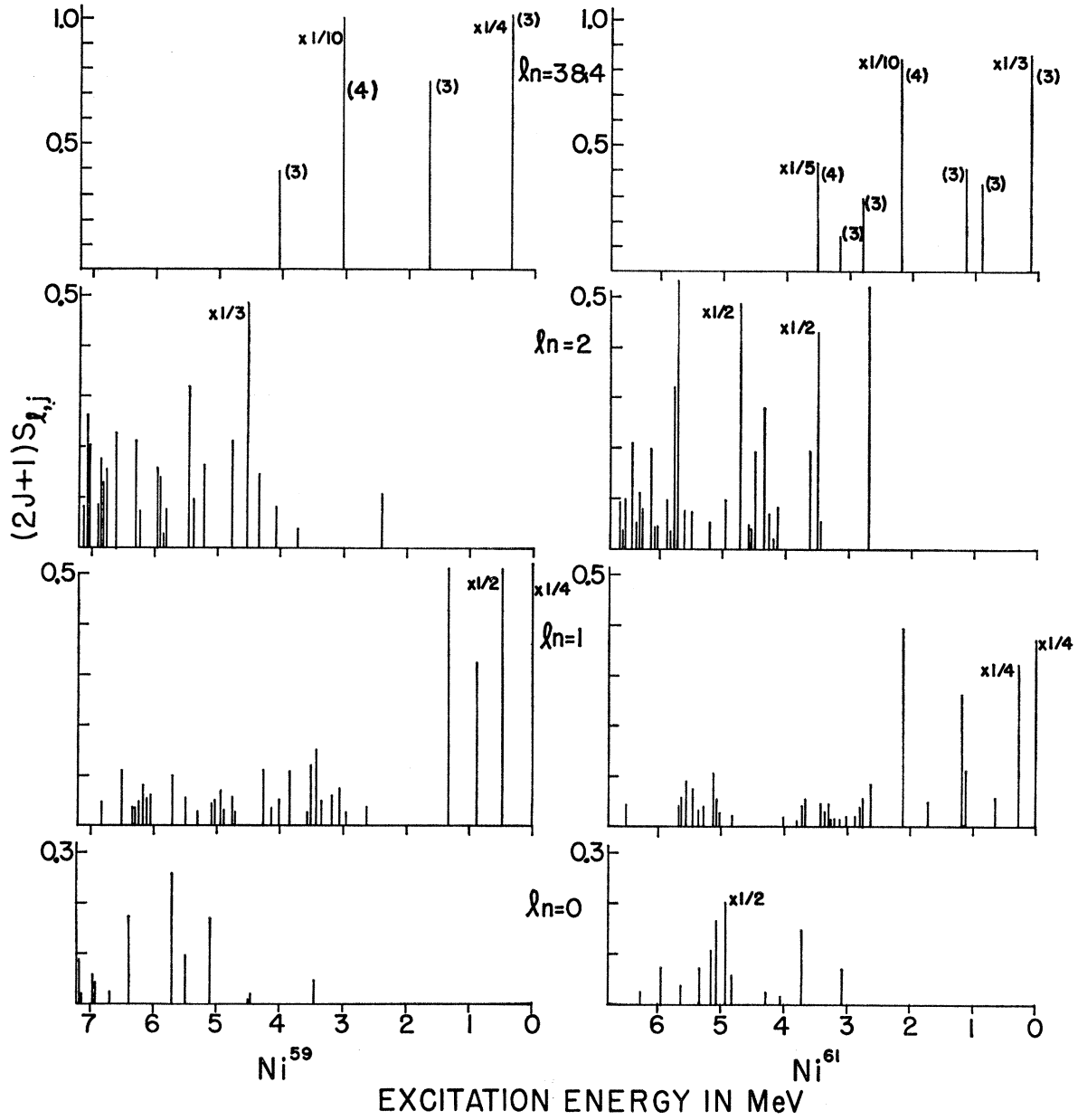

FIG. 9. The spectroscopic strengths $(2J+1)S_{l_n,j}$ for Ni^{59} and Ni^{61} plotted as a function of excitation energy and l_n. The strengths are taken from Ref. 1 and Table I of this paper, respectively.

$\Sigma S_{l_n,j}$ values agree best with pairing theory in case (3b) for the $p_{3/2}-p_{1/2}$ orbits and case (1a) for $f_{5/2}$. However, in view of the possible 30% or more error from approximations made in the DWBA analysis alone, no strong conclusions should be made from such a comparison. It seems evident from the table that any significant spreading of the $\frac{3}{2}^-$ levels to higher excitation would raise $E(p_{3/2})$ and $E(p_{1/2})$ 1 or 2 MeV higher above $E(f_{5/2})$ than is assumed in the pairing-theory calculations of Ref. 2.

B. Comparison of the (d,p) Results with Earlier Work

1. Previous (d,p) Experiments

The earliest (d,p) stripping studies on Ni^{60} were done in this laboratory[11] using a single-gap analyzing magnet to obtain angular distributions. However, because the quality of data is so much improved in the present experiment, we have not included our older results in

[11] R. A. Fisher and H. A. Enge, Bull. Am. Phys. Soc. 4, 287 (1959).

this paper. Fulmer *et al.*[4] have reported the results of an investigation of the $Ni^{60}(d,p)Ni^{61}$ reaction at 12-MeV incident energy. For comparison with our present work, we have listed their results in columns 6, 7, and 8 of Table I. Within the excitation range 0–7.05 in MeV in Ni^{61}, they resolved 94 levels, compared with the 197 levels that were port here. For the levels that have been resolved in both works, the l_n assignments are usually in agreement when the cross sections are large. However, there are a number of disagreements in the cases where the yields are low. In comparing the sum strengths of Fulmer *et al.* with ours in this section, we have taken their uncorrected values, since their corrected numbers involve a normalization that we have not used in our DWBA analysis. Specific comments on the angular-distribution assignments follow.

The $l_n=4$ distributions. In Ref. 4, only one level in Ni^{61} was assigned to be $l_n=4$. This corresponds to our level No. 16 at 2.130 MeV. This strong group appears to be a doublet which fits well with a sum of $l_n=1$ and 4 DWBA curves (Fig. 4). We observe another $l_n=4$ level at 3.492 MeV, and the angular distribution for this state follows the DWBA predictions fairly closely (Fig. 4). The 3.492-MeV state was not observed in Ref. 4, probably because it is only 15 keV from a very strong d state. Our assignments give $\Sigma S=1$ and $E_{9/2}=2.46$ MeV for the $g_{9/2}$ state, compared with $\Sigma S=0.71$ and $E_{9/2}=2.1$ MeV in Ref. 4.

The $l_n=3$ distributions. The comparison of the two experiments for this case is completely summarized by Table IV, and a discussion of specific groups and of the possibility of $f_{7/2}$ hole-state stripping is given there.

As seen in Fig. 4, the distribution Nos. 7, 24, and 29 follow the DWBA $l_n=3$ curves closely near the position of the first forward-angle maximum but depart somewhat elsewhere. Thus, by the conventional criterion, we have assigned them $l_n=3$ in Table I. Since the first forward-angle maximum of No. 4 deviates from the DWBA curve, the assignment is labeled as uncertain: $l_n=(3)$. Because of the large $f_{5/2}$ state at 0.068 MeV, the results in Table III are fairly insensitive to the inclusion of the weaker $l_n=3$'s and are in reasonable agreement with the values of $\Sigma S=0.72$ and $E(f_{5/2})=0.4$ MeV of Ref. 4.

The $l_n=2$ distributions. In the present experiment we report 30 $l_n=2$ distributions up to 6.67 MeV in Ni^{61}. Fulmer *et al.*[4] make 41 $l_n=2$ level assignments in the same region, 21 of which are in agreement with ours. Of the remaining 20 levels, we have assigned four to $l_n=0$, six to $l_n=1$, one to $l_n=(3)$, and nine to ns. In addition, we have assigned $l_n=2$ to three groups given $l_n=0$ assignments in Ref. 4 and to six other groups that Fulmer *et al.* did not resolve.

A speculative division of the $l_n=2$ levels in $j=\frac{5}{2}$ and $j=\frac{3}{2}$ was made by Fulmer *et al.*; however, no such attempt has been made with our data. We only compare the value of $\Sigma(2J+1)S=5.5$ given in Table II for the 30 $l_n=2$ levels found here below 6.67 MeV to the value of 5.97 for the 41 levels in the same region in Ref. 4.

The $l_n=1$ distributions. We have assigned $l_n=1$ to 32 distributions, compared to the 16 reported in Ref. 4. There are 13 agreements, constituting 89% of our total observed strengths. The assignments in Ref. 4 of the other 19 levels are: five with $l_n=2$, one with $l_n=3$, and 13 not resolved.

In both experiments, it appears that the DWBA analysis overestimates the total $2p$ strength [see Table II, cases (a) and (b)]. The possibility of anomalous effects with resultant incorrect assignments is discussed in Sec. III D2.

The $l_n=0$ distributions. Here we report 13 $l_n=0$ transitions, while Fulmer *et al.* find nine. Agreement is found for five strong states, and the remaining eight in this work were either labeled $l_n=2$ or not seen in Ref. 4. Some of these eight states, however, are weak, and their assignments are tentative (see Fig. 4). Here again the difference between stripping and nonstripping patterns is not clear. The questionable states do not affect the sum strength strongly, and both experiments take into

TABLE III. Results of the sum-rule analysis using the fixed-Q approach are shown for the $Ni^{58}(d,p)Ni^{59}$ (Ref. 1) and $Ni^{60}(d,p)Ni^{61}$ reactions. Cases (1a), (2a), and (3a) represent different distributions of $p_{3/2}$ and $p_{1/2}$ assignments among all the observed $l_n=1$ levels, since most of their spins have not been measured. Below the tables are the numbers of levels in Ni^{59} (Table II, Ref. 1) and Ni^{61} (Table I, present work) which were included in the $p_{3/2}$ sums for each of these cases. The remaining $l=1$ levels were taken to be $p_{1/2}$. Cases (1b), (2b), and (3b) use the same distributions of spins but exclude from the sum rules all tentative $l_n=1$ assignments, which are shown in parentheses in the above-mentioned tables. Cases (1a) and (1b) treat the $f_{5/2}$ strength similarly.

		Experiment[a]						Pairing theory[b]	
		$\Sigma S_{l_n,j}$			$E_{l_n,j}$ (MeV)				
$Ni^{58}(d,p)Ni^{59}$		(1)	(2)	(3)	(1)	(2)	(3)	$\Sigma S_{l_n,j}$	$E_{l_n,j}$ (MeV)
$p_{3/2}$	(a)	0.76	0.78	0.81	0.11	1.3	1.9	0.67	0.96
	(b)	0.76	0.78	0.79	0.11	1.3	1.5		
$p_{1/2}$	(a)	1.30	1.18	1.05	3.4[c]	3.4	3.2	0.96	0.96
	(b)	1.28	1.06	0.89	3.2	2.9	2.9		
$f_{5/2}$	(a)	0.88			1.0			0.90	0.34
	(b)	0.79			0.6				
$g_{9/2}$		1.0			3.06			0.99	3.8

Case (1): $p_{3/2}$; 0, 3 and $f_{5/2}$; 1, 7, 56.
Case (2): $p_{3/2}$; 0, 3, 32, 35, 44, 57, 79.
Case (3): $p_{3/2}$; 0, 3, 21, 28, 35, 54, 57, 69, 79, 98, 113, 117, 124.

$Ni^{60}(d,p)Ni^{61}$		Experiment (present work)							
$p_{3/2}$	(a)	0.45	0.48	0.50	0.24	0.79	1.7	0.43	0.0
	(b)	0.45	0.48	0.44	0.24	0.70	1.8		
$p_{1/2}$	(a)	1.25	1.10	1.04	2.6	2.7	2.3	0.90	0.43
	(b)	1.08	0.98	0.89	2.4	2.3	2.6		
$f_{5/2}$	(a)	0.70			0.65			0.76	0.01
	(b)	0.65			0.62				
$g_{9/2}$		1.0			2.46			0.99	3.1

Case (1): $p_{3/2}$; 0, 3, 8 and $f_{5/2}$; 1, 4, 7, 24, 29.
Case (2): $p_{3/2}$; 0, 3, 8, 21, 34, 36, 46.
Case (3): $p_{3/2}$; 0, 3, 8, 21, 27, 34, 36, 46, 58, 105, 107, 115, 122, 130.

[a] Reference 1.
[b] Reference 2.
[c] In Table V of Ref. 1, this was incorrectly written as 2.4 MeV.

TABLE IV. Comparison of (d,p), (p,d), (d,t), and (He^3,α) reactions leading to levels in Ni^{59} and Ni^{61}. Shown here are only those parts of the data relevant to the identification of $\frac{5}{2}^-$ and $\frac{7}{2}^-$ levels in these two nuclei.

	$Ni^{58}(d,p)Ni^{59}$ Ref. 1		$Ni^{58}(d,p)Ni^{59}$ Ref. 4		$Ni^{60}(p,d)Ni^{59}$ Ref. 5		$Ni^{60}(d,t)Ni^{59}$ Ref. 12		$Ni^{60}(He^3,\alpha)Ni^{59}$ Ref. 13	
Level	E_x (MeV)	l_n	E_x (MeV)	l_n	E_x (MeV)	j^π	E_x (MeV)	j^π	E_x (MeV)	j^π
1	0.341	3	0.340	3	0.33	$\frac{5}{2}^-$			0.34	$\frac{5}{2}$
7	1.685	3	1.696	(3)						
11	1.953	ns	1.967	...	1.96	$\frac{7}{2}^-$	1.98	...	1.97	$(\frac{5}{2},\frac{7}{2})$
14	2.533	ns								
15	2.633	(1)	2.640	3	2.63	$\frac{7}{2}^-$	2.65	$\frac{7}{2}^-$		
16	2.683	ns	2.698	...						
17	2.692	ns							2.70	$\frac{7}{2}^-$
18	2.705	ns								
19	2.718	ns								
20	2.901	(1)	2.910	1						
21	3.035	(1)	3.045	1	3.04	$\frac{7}{2}^-$				
23	3.132	ns	3.151	...			3.09		3.15	$\frac{7}{2}^-$
40	3.728	ns								
41	3.745								3.74	$\frac{7}{2}^-$
42	3.791	ns								
55	4.177	ns								
56	4.213	(3)	4.210	2	4.17	$(\frac{7}{2}^-)$				

	$Ni^{60}(d,p)Ni^{61}$ Present work		$Ni^{60}(d,p)Ni^{61}$ Ref. 4		$Ni^{62}(p,d)Ni^{61}$ Ref. 5		$Ni^{62}(d,t)Ni^{61}$ Ref. 12	
Level	E_x (MeV)	l_n	E_x (MeV)	l_n	E_x (MeV)	j^π	E_x (MeV)	j^π
1	0.068	3	0.069	3	0.068	$\frac{5}{2}^-$		
4	0.916	(3)	0.908	3				
7	1.139	3	1.139	3	1.17	...		
9	1.462	ns	1.454	3	1.46	$\frac{7}{2}^-$	1.45	$(\frac{7}{2}^-)$
13	1.996	ns						
14	2.009	ns			(2.07)	$(\frac{7}{2}^-)$	2.00	$(\frac{7}{2}^-)$
15	2.025	ns						
17	2.417	ns						
18	2.474	ns	2.473	(2)	2.47	$(\frac{7}{2}^-)$	2.48	...
19	2.536	ns	2.533					
26	2.910	(1)	2.910	2	2.90	$\frac{7}{2}^-$	2.92	$\frac{7}{2}^-$
27	3.051	(1)						
29	3.116	3	3.127	(2)			3.13	...
33	3.268	(1)						
34	3.308	(1)	3.305	(3)	3.28	$\frac{7}{2}^-$	3.31	$\frac{7}{2}^-$

account only 50% of the $3s_{1/2}$ strength below 6.8 MeV in Ni^{61}.

It may be that some of the discrepancies in the results of the two experiments are due to effects dependent upon incident energy, since Fulmer *et al.* used $E_d=12$ MeV and the present work was done at $E_d=7.5$ MeV (see Sec. III B2). However, several examples of levels in Table I indicate the possibility of misinterpretation and point to the importance of good resolution and complete angular distributions.

2. *Pickup Data*

In principle, single-neutron-stripping and pickup data should give quantitative information on the degree of vacancy U_j and occupancy V_j, respectively, for an orbit j in the same target nucleus[3] with the consistency that $U_j^2+V_j^2=1$. In practice, however, the DWBA analyses alone may have such large uncertainties that it becomes difficult to make a meaningful comparison of these quantities. Nevertheless, we have used our fixed Q-value results of Table III (with $U_j^2=S_j$) and the V_j^2's from (d,t) pickup data of Fulmer and Daehnick[12] to determine the above sum for the $p_{3/2}$, $p_{1/2}$, and $f_{5/2}$ orbits in Ni^{58} and Ni^{60}. We took the values of V_j^2 in Ref. 11 that also were calculated using a fixed Q-value procedure. For the cases given in Table III, the sum $U_j^2+V_j^2$ for the $p_{3/2}$, $p_{1/2}$, and $f_{1/2}$ states in Ni^{58} range from 1.03 to 1.08, 1.02 to 1.43, and 0.99 to 1.00, respectively; and in Ni^{60} from 1.00 to 1.06, 1.22 to 1.58, and 0.83 to 0.88, respectively. The over-all consistency is seen to be good, and the deviations from unity are well within the limits of the uncertainties in the DWBA analysis.

The combination of pickup data and high-resolution (d,p) data should yield information on the question of possible nonclosure of the $f_{7/2}$ shell in the Ni^{58} and Ni^{60} ground states. For example, weak $l_n=3$ transitions in $Ni^{60}(d,p)Ni^{61}$ to states expected to be $\frac{7}{2}^-$ from $Ni^{62}(p,d)Ni^{61}$ would indicate the presence of $f_{7/2}$ holes in $Ni^{60}(0)$. A summary of all relevant data currently available in the literature is given in Table IV. From this table, it will be noted that there are several factors which

[12] R. H. Fulmer and W. W. Daehnick, Phys. Rev. **139**, B579 (1965).

complicate the comparison. The first is that there is no clear correspondence between the levels seen in our (d,p) reaction and those from pickup. For example, in the case of the $\frac{7}{2}^-$ state at about 2.65 MeV in Ni^{59}, there are five or six states seen here within the range of possible energies for this state given in Refs. 5, 12, and 13. It may be that one or more of these states are $\frac{7}{2}^-$ and that pickup experiments have not resolved them all (see Sec. III D).

Secondly, in the (d,p) results there are uncertainties in the l_n assignments that preclude definite conclusions. Several such cases in Ni^{59} were already mentioned in Ref. 1. In Ni^{61} we cite levels Nos. 26 and 27 and Nos. 33 and 34 as examples (see Fig. 5). If we judge only from position of the first forward-angle maximum, an unbiased assignment is $l_n=(1)$ for these levels. However, the DWBA curve fits poorly for all but these few forward angles. If the spins here are actually $\frac{7}{2}^-$, then at this incident energy the conventional approach to determining l_n values is in error. Level No. 9 in Ni^{61} is another interesting example. Here the level is well isolated and is given a definite assignment of $j^\pi=\frac{7}{2}^-$ in Ref. 5. Its angular distribution, designated "ns" does not resemble any typical stripping shape, but it is identical to that of No. 11 in Ni^{59} (see Fig. 11), which was also given $\frac{7}{2}^-$ from pickup data. Fulmer *et al.*[4] have indicated $l_n=3$ for No. 9 from their (d,p) work at $E_d=12$ MeV. However, they have not made an assignment for the counterpart, No. 11 in Ni^{59}. This is one of several examples in Table IV of disagreement between the two (d,p) experiments.

In summary, therefore, there is no unambiguous case from our data to suggest stripping to holes in the $Ni^{58}(0)$ or Ni^{60}. Level No. 56 in Ni^{59} seems the most hopeful candidate by the usual DWBA guidelines. However, its assignment is tentative, and its energy does not correspond so closely to the 4.17 $(\frac{7}{2}^-)$ state of the (p,d) data as the "ns" level No. 55.

As in Ref. 1, we can suggest two possible explanations for the behavior of the (d,p) distributions in the above cases:

1. The $\frac{7}{2}^-$ states seen in the pickup reactions may be core-excited states that cannot be populated directly by stripping but must be populated by higher-order processes. Therefore, the (d,p) distributions show ns or irregular patterns.

2. The other alternative is that the transitions correspond to the filling of holes in the Ni^{58} and Ni^{60} ground states, but at this bombarding energy such $f_{7/2}$ hole-state stripping gives rise to anomalous distributions, unlike the conventional shapes for $l_n=3$ transfers. In this case, the $l_n=3$ assignment to level No. 15 in Ni^{59} and to No. 9 in N^{61}, given by Fulmer *et al.*,[4] with $E_d=12$ MeV, could imply that the DWBA calculation is only valid for such hole-state stripping at higher incident energies.

[13] C. M. Fou, R. S. Zurmühle, and L. E. Swenson, Phys. Rev 144, 927 (1966).

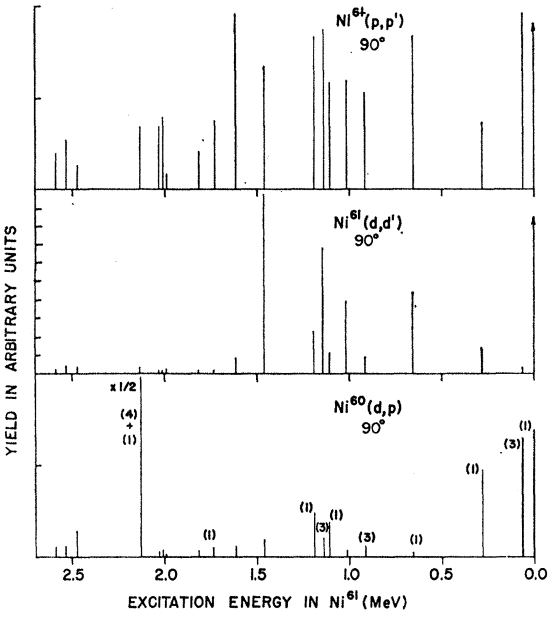

FIG. 10. The 90° yields from the three reactions studied are plotted here as a function of excitation energy in Ni^{61}.

In either case, the $\frac{7}{2}^-$ strength may be spread over a number of weaker states, which, from our results, seem to cluster around the energies located in Refs. 5, 12, and 13 (see Fig. 10 and Sec. III D), and which might be identified individually with higher-resolution pickup data.

C. The Low-Lying Levels in Ni^{61}

Although only two spins have previously been measured[6] in Ni^{61}, namely, $\frac{3}{2}^-$ for the ground state and $\frac{1}{2}^-$ at $E_x=0.284$ MeV, there are a large number that can be inferred from reaction information as summarized in the following. Using the indications of the Lee-Schiffer dips in $l_n=1$ transitions of our (d,p) data, we make the following tentative assignments: $\frac{3}{2}^-$ at 0.661 and 1.192 MeV, and $\frac{1}{2}^-$ at 1.106 and 1.737 MeV. These dips are not very pronounced and become even less so at higher excitations. Matching the four strongest $l_n=1$ transitions of Ni^{59} and Ni^{61} (see Fig. 9) and from known spins in Ni^{59}, we believe that the Ni^{61} level at 2.130 MeV is most probably $\frac{3}{2}^-$ also. The results of (p,d) and (d,t) experiments[5,12] give $\frac{5}{2}^-$ to the level at 0.068 MeV, and, from the low yields of these reactions to the $l_n=3$ levels seen here at 0.916, 1.139, 2.804, and 3.116 MeV, we tentatively suggest a spin assignment of $\frac{5}{2}^-$ to these levels as well. In addition, the pickup data in Refs. 5 and 12 indicates $\frac{7}{2}^-$ to states in the vicinity of 1.46, 2.00, 2.47, 2.91, and 3.30 MeV. Finally, by simple shell-model reasoning, we expect the states at 2.130 and 3.492 MeV to be $\frac{9}{2}^+$ in view of the $l_n=4$ stripping patterns for these states.

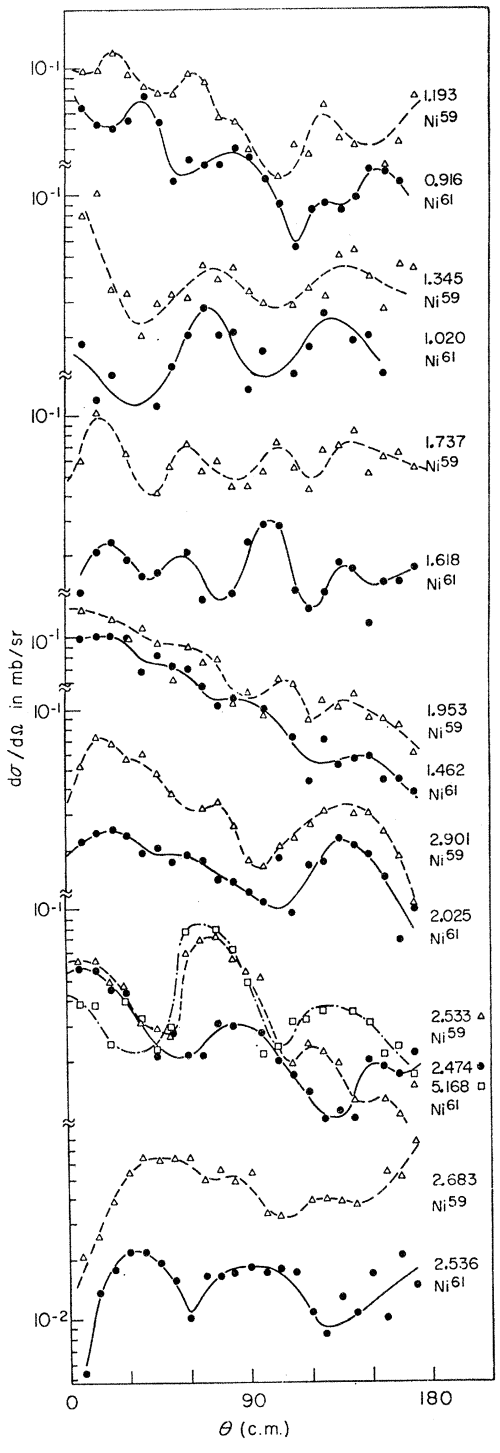

FIG. 11. Several nonstripping angular distributions from the $Ni^{58}(d,p)Ni^{59}$ and $Ni^{60}(d,p)Ni^{61}$ reactions are compared. The excitation energies for the corresponding states in Ni^{59} and Ni^{61} are indicated to the right of each curve. The solid lines are just visual guides through the data points. Similarities in shapes from the two reactions appear to be present and point to the possible usefulness of such weak transitions in classifying states in the final nucleus.

To extract nuclear-structure information on Ni^{61} from our (d,d') results, it would be desirable to carry out a DWBA analysis. In order to perform such an analysis, it is necessary to have more nuclear-model data or assumptions as input information than in the usual (d,p) case. The two different approaches that have been taken in previous nuclear-model calculations are, first, a particle-plus-phonon model[3] and, second, a shell-model picture involving only the neutrons outside the $f_{7/2}$ core.[2] Similar descriptions might then be incorporated into the treatment of the (d,d') reaction mechanism. In the calcium isotopes, for example, this has been carried out to test the validity of these models in that region.[14] Since no such analyses of our (d,d') data have yet been performed, we must restrict ourselves here to more qualitative remarks on the present results.

Figure 10 shows the comparative yields at 90 deg from the three reactions we have studied. The (p,p') reaction is very nonselective, as expected from a compound-nuclear mechanism (see Sec. II A). In the (d,d') reaction, excluding the elastic group, there are nine transitions, Nos. 2–10, that have distinctively larger yields than do the others, and, in addition from Fig. 3, we see that six (or seven if No. 10 is included) are characterized by a total orbital angular-momentum transfer of $L=2$. The remaining two, Nos. 2 and 6, have been given tentative $\frac{3}{2}^-$ spins in the preceding discussion and these display identical (d,d') angular distributions. For these assignments, only $L=0$ and 2 transfers could be involved; however, spin effects probably are important in the excitation process. From the figure, we see that six of the nine states prominent in (d,d') are also populated by direct stripping, but that generally those transitions that are strong in the (d,p) reaction are weak in the (d,d'), and vice versa.

In a particle-plus-phonon model the $p_{3/2}$ ground-state neutron is coupled to the first 2^+ vibration in Ni^{60} and a multiplet of states with spins $\frac{1}{2}^-$, $\frac{3}{2}^-$, $\frac{5}{2}^-$, and $\frac{7}{2}^-$ is formed in Ni^{61}. This would be at best an approximation, since it neglects the exclusion principle, which, for example, does not allow a $(p_{3/2})^2$ 2^+ component of the 2^+ phonon to couple with another $p_{3/2}$ neutron to form $\frac{7}{2}^-$. Furthermore, it may be that this multiplet of states is strongly admixed with other nearby configurations, such as $(f_{5/2}\times 2^+)_J$ and the pure $2p$ and $f_{5/2}$ single-particle states, so that the $(p_{3/2}\times 2)_J$ strength is spread over more than four levels. Thus, the usual center-of-gravity and $(2J+1)$ intensity rules derived for this model[15] may not apply. In fact, we have been unsuccessful in getting reasonable agreement between our relative (d,d') yields and the predictions of this intensity rule for any arrangement of transitions. However, it is interesting to note that the sum of the yields to the nine states in Ni^{61} that are dominated by $L=2$ transfers is nearly

[14] T. A. Belote, J. H. Bjerregaard, Ole Hansen, and G. R. Satchler, Phys. Rev. 138, B1067 (1965).

[15] F. Perey, R. J. Silva, and G. R. Satchler, Phys. Letters 4, 25 (1963).

identical to the yield to the $Ni^{60}(2^+)$. The data for the latter were obtained simultaneously in our experiment because of a small Ni^{60} contamination in the Ni^{61} target (see Sec. II A). This agreement might be expected if the vibrational model is valid, and the (d,d') strength is simply a measure of the $(p_{3/2}\times 2^+)_J$ admixture in a residual-state wave function. It is also interesting that the strongest $Ni^{61}(d,d')$ transition is to the 1.462-MeV state which has been determined to be a $\frac{7}{2}^-$ core-excited state by pickup reactions.[5,12] If this state is constructed from excitations similar to those in the $Ni^{60}(2_1^+)$ state, then this would imply that $f_{7/2}$ particle excitations should be included in a description of the lowest 2^+ wave function in Ni^{60}.

Some information on the lowest odd-parity vibrations in Ni^{58} and Ni^{60} might also be obtained from the results of our (d,p) studies in Ref. 1 and in the present work. In particular, the fragmentation of the $g_{9/2}$ strength in Ni^{59} and Ni^{61} could be thought to arise from the mixing of the $g_{9/2}$ particle state with $\frac{9}{2}^+$ states formed by coupling $p_{3/2}$ or $f_{5/2}$ particles to the lowest known 3^- vibrations in Ni^{58} and Ni^{60} at $E^{58}(3^-)=4.5$ MeV and $E^{60}(3^-)=4.04$ MeV.[16–18] In a weak-coupling approximation, it might be expected that the degree of mixing would be inversely proportional to the difference in excitation energies of the 3^- and $g_{9/2}$ states in the neighbor nuclei. Using our values from Table III, we have $E^{58}(3^-)-E^{59}(g_{9/2})=1.44$ MeV and $E^{60}(3^-)-E^{61}(g_{9/2})=1.58$ MeV, and therefore the above argument appears inadequate to account for the strong splitting of the $g_{9/2}$ strength in Ni^{61} but not in Ni^{59}. A possible alternative explanation might be the presence of another odd-parity vibration in Ni^{60} below the known 3^- state at 4.04 MeV. Actually, such a state was seen by Jolly[17] at $E_x=3.13$ MeV and was assigned $J^\pi=3^-$, which is compatible with this explanation. However, other sources of data seem to refute the existence of this state.[15]

The exclusion principle should not prohibit configurations in Ni^{61} involving particles coupled with the neighboring 3^- of Ni^{60}, and a search for these at around 2.5- to 5-MeV excitation with the (d,d') reaction would have been interesting. However, our yields were too low there to gain any such information.

D. The Nonstripping (d,p) Transitions and Intermediate Structure

It is evident from Fig. 7 that many of the (d,p) angular distributions that have been called nonstripping patterns have a well-defined oscillatory character. It might be hoped, therefore, that, with enough data, systematic similarities might be recognized and useful information extracted from them. Within groups of states shown in Fig. 7, a number of such similarities can be identified. Furthermore, several likenesses in these patterns have been seen between the $Ni^{58}(d,p)Ni^{59}$ and the $Ni^{60}(d,p)Ni^{61}$ reactions, some examples of which are presented in Fig. 11. In the uppermost case, we draw an analogy between level No. 4 of Ni^{59} assigned ns and No. 4 of Ni^{61}, which is rather poorly fitted with an $l_n=3$ DWBA curve. This illustrates what seems to be a transition from a clearly nonstripping state to a

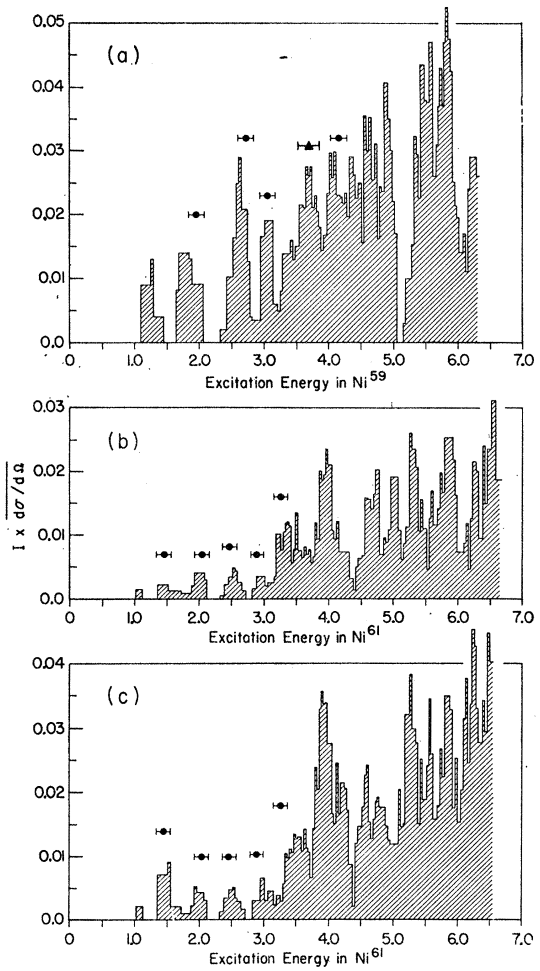

FIG. 12. Strength functions determined by averaging the cross sections for both the nonstripping states and the weak and questionable $l_n=1$ transitions determined from the $Ni^{58}(d,p)Ni^{59}$ reaction (Ref. 1) and from the $Ni^{60}(d,p)Ni^{61}$ reaction [Figs. 1(b) and 1(c)]. Two different procedures were tried. In Figs. 1(a) and 1(c), the quantity

$$Id\sigma/d\Omega(E,I,60°)=\sum_{E-I<E'\leq E+I} d\sigma/d\Omega(E',60°)$$

is plotted against E, where the sum is over the above-mentioned classes of levels, $I=0.1$ MeV, and E is taken in steps of 0.33 MeV. The second procedure, represented in Fig. 1(b), replaced the summand in the above relationship with the average cross section for laboratory angles greater than 90 deg. This was done only for the $Ni^{60}(d,p)Ni^{61}$ reaction because of the greater availability of data in the back angles. The circles above the graphs represent the positions of $f_{7/2}$ hole states determined by (p,d) and (d,t) pickup reactions (Refs. 5 and 12) and the triangle above the Ni^{59} plot locates an additional $f_{7/2}$ hole state found in $Ni^{60}(He^3,\alpha)Ni^{59}$ pickup (Ref. 13). The horizontal bars on these dots indicate the experimental energy uncertainty for these positions.

[16] B. L. Cohen, Phys. Rev. **130**, 227 (1963).
[17] R. K. Jolly, Phys. Rev. **139**, B318 (1965).
[18] S. M. Shafroth and G. T. Wood, Phys. Rev. **149**, 827 (1966).

weak stripping state arising from the increased single-particle damping in Ni^{61}. Another interesting case is level No. 11 of Ni^{59} at 1.953 MeV and No. 9 of Ni^{61} at 1.462 MeV, both of which were assigned $\frac{7}{2}^-$ from (p,d) pickup[11] and which have identical ns distributions in the (d,p) reaction.

Recently, it has been suggested by Bolsterli *et al.*[19] that positions of two-particle, one-hole $(2p\text{-}1h)$ configurations with respect to a target nucleus can be found by looking at the strength function of nonstripping levels from the (d,p) reaction on that target. The surmise is that the (d,p) reaction might enhance these excitations that are the next order of complexity after the single-particle components and that there should be clustering of levels around such configurations with widths of the order of 100 keV. The problem of sorting out such $2p\text{-}1h$ strengths from the more prominent single-particle amplitudes is an obvious difficulty of the method. We have made an attempt to do this here in the $Ni^{58}(d,p)Ni^{59}$ and $Ni^{60}(d,p)Ni^{61}$ cases, where in the latter we used two different procedures. The most successful of these considered the average back-angle cross sections for the nonstripping transitions, as well as the weak stripping distributions that show obvious deviations from DWBA shapes and for which the l_n assignment is questionable. Hopefully, in the latter case, this will give some measure for the amount of more complicated configurations admixed with the single-particle amplitude. The results are shown in Fig. 12, and the averaging procedure is described in the caption. Some structure does seem to exist in these graphs, although it becomes more obscure at higher excitations. In the figure are also the locations of possible $\frac{7}{2}^-$ hole states determined by Sherr *et al.*[5] and by Fou *et al.*[13] from pickup reactions, and they do correspond in most cases to enhancements of the nonstripping strength function.

Each enhancement shown usually arises from several weak and closely spaced nonstripping states. Therefore, these states might be thought to share the strength of a $(2p\text{-}1h)$ configuration in the vicinity of their average excitation energy. In the cases corresponding to $f_{7/2}$ core-excited states, this would mean that the pickup experiments of Refs. 5, 12, and 13, if performed with higher resolution, would have uncovered a multiplet of $\frac{7}{2}^-$ states at the positions shown in Fig. 12.

[19] M. Bolsterli, W. R. Gibbs, A. K. Kerman, and J. E. Young, Phys. Rev. Letters **17**, 878 (1966).

ACKNOWLEDGMENTS

The authors are indebted to Professor W. W. Buechner for his guidance in this work and for initiating the early investigations on nickel in this laboratory. We also gratefully acknowledge the stimulating interest of Professor A. K. Kerman. The discussions with Dr. Ole Hansen and M. Veneroni in the beginning stages of our work are greatly appreciated. The DWBA computations were done by H. Y. Chen at the MIT Computation Center, and the scanning was expertly carried out by W. A. Tripp, Miss Sylvia Darrow, and Mrs. Mary Fotis. We extend our thanks to Mrs. Mary E. White for her assistance during the preparation of the manuscript.